ARTICLE IN PRESS

+ MODEL

Available online at www.sciencedirect.com

ScienceDirect

Green Energy & Environment xxx (xxxx) xxx



www.keaipublishing.com/gee

Research paper

Zeolite-templated carbons as effective sorbents to remove methylsiloxanes and derivatives: A computational screening

Shiru Lin ^{a,1}, Kaitlyn A. Jacoby ^{b,1}, Jinxing Gu ^a, Dariana R. Vega-Santander ^c, Arturo J. Hernández-Maldonado ^{c,**}, Zhongfang Chen ^{a,*}

a Department of Chemistry, University of Puerto Rico, Río Piedras, San Juan, PR 00931, USA
 b Department of Chemistry & Biochemistry, Elizabethtown College, Elizabethtown, PA 17022, USA
 c Department of Chemical Engineering, University of Puerto Rico, Mayagüez Campus, Mayagüez, PR 00681, USA

Received 4 March 2020; revised 7 July 2020; accepted 8 July 2020

Available online ■■■

Abstract

Though widely used in our daily lives, volatile methylsiloxanes and derivatives are emerging contaminants and becoming a high-priority environment and public health concern. Developing effective sorbent materials can remove siloxanes in a cost-effective manner. Herein, by means of Grand Canonical Monte Carlo (GCMC) simulations, we evaluated the potentials of the recently proposed 68 stable zeolite-templated carbons (ZTCs) (PNAS 2018, I15, E8116-E8124) for the removal of four linear methylsiloxanes and derivatives as well as two cyclic methylsiloxanes by the calculated average loading and average adsorption energy values. Four ZTCs, namely ISV, FAU1, FAU3, and H8326836, were identified with the top 50% adsorption performance toward all the six targeted contaminants, which outperform activated carbons. Further first principles computations revealed that steric hindrance, electrostatic interactions (further enhanced by charge transfer), and CH- π interactions account for the outstanding adsorption performance of these ZTCs. This work provides a quick procedure to computationally screen promising ZTCs for siloxane removal, and help guide future experimental and theoretical investigations.

© 2020, Institute of Process Engineering, Chinese Academy of Sciences. Publishing services by Elsevier B.V. on behalf of KeAi Communications Co., Ltd. This is an open access article under the CC BY-NC-ND license (http://creativecommons.org/licenses/by-nc-nd/4.0/).

Keywords: Zeolite-templated carbons; Contaminants of emerging concern; Methylsiloxanes; GCMC simulations; Density functional theory calculations

1. Introduction

As a type of critical organic compounds, methylsiloxanes [1–7] are used in many industries and consumer products, including oil production [8], dry cleaning, personal care products [9], and the manufacturing of higher weight silicon polymers [4]. Methylsiloxanes contain methyl substituents bonded to the silicon atoms of an alternating silicon-oxygen backbone, which can be in the cyclic or linear form [10].

E-mail addresses: arturoj.hernandez@upr.edu (A.J. Hernández-Maldonado), zhongfangchen@gmail.com (Z. Chen).

For instance, decamethylcyclopentasiloxane (D5) and octamethylcyclotetrasiloxane (D4) are the most prevalent cyclic volatile methylsiloxanes (cVMS) in the environment [11–15]. The other containments, monomethylsilanetriol (MMST) [16], dimethylsulfone (DMSO₂) [17–19], trimethylsilanol (TMS), as well as dimethylsilanediol (DMSD) [20,21] are the smallest linear methylsiloxanes and derivatives [19,22,23], which are commonly found after the hydrolysis and sulfuration of longer linear and cyclic methylsiloxanes.

Though methylsiloxanes play essential roles in our lives, the treatment and discharge of methylsiloxanes are still challenging. The US alone produced 100–500 million pounds of D4 and 50–100 pounds of D5 in 2006 [24] and released about 10 million kilograms of methylsiloxanes in general per year [25]. However, because methylsiloxanes are hydrophobic and

https://doi.org/10.1016/j.gee.2020.07.007

2468-0257/© 2020, Institute of Process Engineering, Chinese Academy of Sciences. Publishing services by Elsevier B.V. on behalf of KeAi Communications Co., Ltd. This is an open access article under the CC BY-NC-ND license (http://creativecommons.org/licenses/by-nc-nd/4.0/).

^{*} Corresponding author.

^{**} Corresponding author.

¹ These authors contributed equally to this work.

2

often highly volatile, the removal of methylsiloxanes is very difficult [26–31]. Moreover, methylsiloxanes have potential toxicity, for example, D4 is toxic to some aquatic life [32], and D5 in the soil can cause adverse effects in certain animal and plant species [9]. Therefore, finding an efficient method for removing methylsiloxanes is urgent.

The traditional separation and purification methods include distillation, crystallization, adsorption, membrane processes, absorption and stripping, and extraction, among which adsorption is a low-cost and the principal method [33,34] for the removal of different methylsiloxanes [5]. Wastewater treatment plants have been applied to decrease the number of methylsiloxanes, but cannot avoid methylsiloxanes residues of a low concentration and the production of smaller silanols or methyl sulfones due to the side reactions of methylsiloxanes [35,36]. Activated carbons are general adsorbents for many contaminants [10], but the pore size, functional group, and metal content of activated carbons cannot be easily characterized and well-controlled compared with some other porous materials [10]. Other commonly used adsorbents are zeolites [8,9], which possess various but regular pore structures, and can be designed to adsorb specific contaminants [37,51].

Recently, zeolite-templated carbons (ZTCs) emerged as promising sorbents. ZTCs can be synthesized cheaply and on a large scale by chemical vapor deposition of carbon over a zeolite template [38-40]. After the carbon forms a structure covering the surface of the pores of zeolite, the zeolite structure can be removed, leaving a porous carbon structure. Several ZTCs have been successfully synthesized with various zeolites as templates, including the FAU, EMT, and LAY zeolites [41,42]. For instance, in 2017, Lee et al. demonstrated that the electrical conductivity of the LAY-templated carbon is related to the degree of order for the pores and also the treatment temperature for synthesizing ZTCs [41]; In 2018, Braun et al. developed a theoretical framework to generate a ZTC model from any given zeolite structure, established criteria for which zeolites can produce experimentally accessible ZTCs, and identified 68 stable ZTCs structures [42].

As a new type of carbon material, ZTCs have a better-controlled pore structure than activated carbons because of the zeolite template used during synthesis processes [41–47]. Note that one drawback of the activated carbons is the decreased adsorption capability toward contaminants during usage because the hydrophilic sites (the functional groups hanging on the activated carbons) tend to adsorb water and alkali metals. In stark contrast, ZTCs are hydrophobic, thus it can be a better choice as adsorbents for methylsiloxanes and derivatives.

In this work, we employed Grand Canonical Monte Carlo (GCMC) simulations to evaluate the adsorption performance of the 68 stable ZTCs recently identified by Braun et al. [42] toward four linear methylsiloxanes and two cyclic methylsiloxanes in terms of average loading and average adsorption energy values. We identified four promising ZTCs, namely ISV, FAU1, FAU3, and H8326836, which have top 50% adsorption performances toward all the six critical methylsiloxanes and are expected to outperform activated carbons. To

gain insights into adsorption mechanisms at the atomistic level, we examined the interactions of the best-performing ZTC toward each contaminant by means of density function theory (DFT) computations and found that steric hindrance, electrostatic interactions, and CH- π interactions play critical roles in enhancing the adsorption capability of these ZTCs.

2. Computational methods

Grand Canonical Monte Carlo (GCMC) simulations were performed using the Sorption module of Materials Studio 8.0 [48] to investigate the absorption performance of 68 ZTCs toward each of the six contaminants. GCMC is a statistical simulation, which evaluates the adsorption process relying on random sampling and probabilistic interpretation in the sorbent framework. We calculated the average adsorption loading (per 10 nm³) (converted from the number of molecules per cell, see Table S1 in Supporting Information) and adsorption energy (kcal mol⁻¹) for which the 10 lowest-energy adsorption geometries of each adsorption system were chosen. Note that a more substantial adsorption loading and higher adsorption energy indicate better adsorption performances. Fixed pressure adsorption simulations were carried out at a temperature of 298 K and a pressure of 101.33 kPa with the Metropolis Monte Carlo method [49] and COMPASS forcefield [50,51]. Using COMPASS forcefield, the carbon atoms of ZTCs were assigned as different types: namely c3a and c3 =, which are used for sp² carbons in typical double bonds and for sp² carbons in aromatic rings, respectively. Considering that no metal atoms were included in our systems, we used the Forcefield assigned charges by COMPASS. Adsorption isotherms were calculated using Sorption codes with the same method and forcefield, but at a pressure range from 1 to 30 MPa.

DFT computations were carried out by using an all-electron method within a generalized gradient approximation (GGA) for the exchange-correlation term, as implemented in the DMol³ code [52,53] for the optimization of six contaminants and further examination of the interactions between the bestperforming ZTC with contaminants. The structures of ZTCs downloaded from materials cloud have been optimized by DFT computations [41]. Also, the structure of all methylsiloxanes were optimized by DFT functional. The double numerical plus polarization (DNP) basis set and Perdew, Burke and Ernzerhof (PBE) functional were adopted [54]. Self-consistent field (SCF) computations were performed with a convergence criterion of 10^{-6} a.u. To obtain more accurate ISV-contaminant interactions, we took long-range electrostatic interaction into account, and adopted DFT + D (D stands for dispersion) vdW correction using Grimme method [55].

3. Results and discussion

3.1. Searching the best ZTC toward each containment

We first explored the performances of ZTCs in adsorbing four linear methylsiloxanes and derivatives (Fig. 1, Table 1,

+ MODEI

S. Lin et al. / Green Energy & Environment xxx (xxxx) xxx

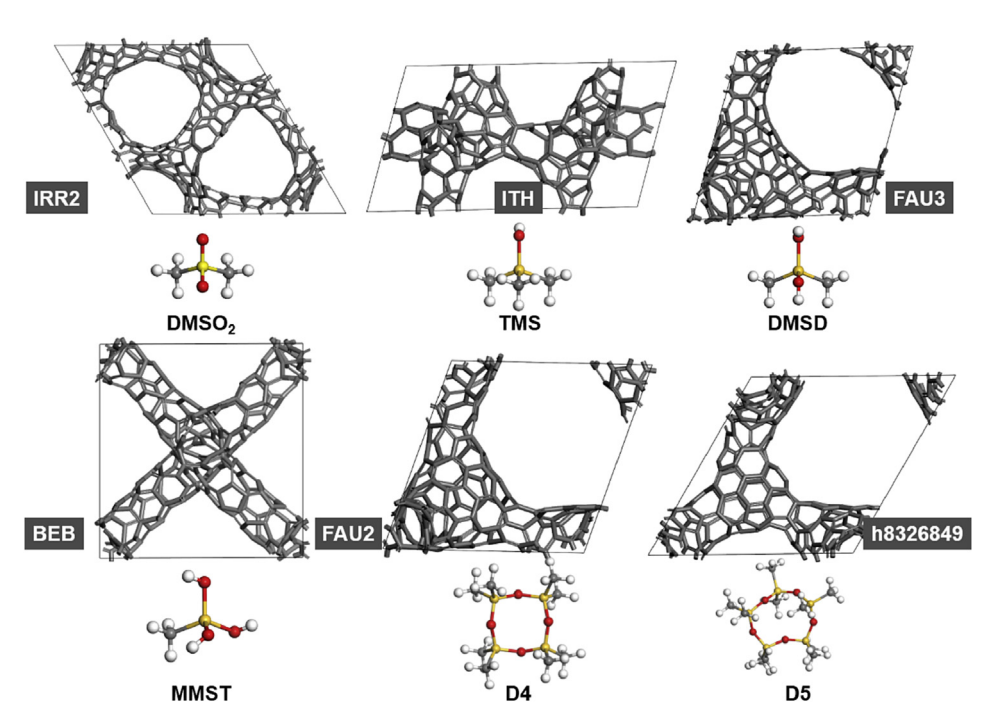


Fig. 1. The structures of four linear siloxanes and derivative as well as two cyclic siloxanes, and the structure of the best ZTC sorbent toward each contaminant. The ZTCs are presented as gray stick models. The yellow, red, earth yellow (only in DMSO₂), and white balls stand for silicon, oxygen, sulfur (only in DMSO₂) and hydrogen atoms, respectively.

Table 1 The best-performed ZTCs for each methylsiloxane and derivative, and the corresponding average loadings (L; per 10 nm³) and average adsorption energies (E; kcal mol⁻¹).

	Best ZTC	L per 10 nm ³	E kcal mol ⁻¹	
DMSO ₂	IRR2	31.26	20.10	
TMS	ITH	26.26	18.47	
DMSD	FAU3	32.25	17.64	
MMST	BEB	33.85	18.92	
D4	FAU2	9.87	38.15	
D5	H8326849	6.20	37.98	

Table S2-S5). The best ZTCs and their performance toward each of these four contaminants are summarized in Fig. 1 and Table 1. Note that typically conventional adsorbents have rather low adsorption energy toward these linear contaminants, thus though both adsorption energies and loading capacities are considered when evaluating the adsorption performance of ZTCs, here we pay more attention to the average adsorption energy. The best sorbent toward a linear contaminant is of the highest adsorption energy among those with decent loading values (top 30% in this work; Table S6-S9).

The best ZTC for adsorbing DMSO₂ is IRR2, which has the seventh-highest adsorption energy value of 20.10 kcal mol⁻¹, and its loading value (31.26 per 10 nm³) is much higher than those with even higher adsorption energies. Another ZTC, namely ISV, also performs well as a sorbent toward DMSO₂, with both adsorption energy and loading in the top 30%.

For TMS, the best ZTC is the ITH structure, which performed in the top 25% for both adsorption energy

(18.47 kcal mol⁻¹) and loading (26.26 per 10 nm³), followed by BEC which possesses both adsorption energy (18.69 kcal mol⁻¹) and loading (24.45 per 10 nm³) in the top 30%.

For DMSD, FAU3 structure performs in the top 25% for both adsorption energy (17.64 kcal mol⁻¹) and loading (32.25 per 10 nm³), and the BEB structure has a little higher energy (17.72 kcal mol⁻¹) than FAU3, but its loading (32.25 per 10 nm³) is only in the top 50% among ZTCs.

For MMST, more ZTC structures have loading and adsorption energy values in the top 30% compared with the other methylsiloxanes. Among them, BEB is the best with the relative highest adsorption energy (18.92 kcal mol⁻¹) with a loading of 33.85 per 10 nm³, immediately followed by ITH (adsorption energy 18.19 kcal mol⁻¹; loading 33.85 per 10 nm³).

Then, we examined the adsorption of ZTCs toward two cyclic methylsiloxanes, namely D4 and D5 (Fig. 1, Table 1, Tables S10 and S11). Compared with their linear counterparts, the 68 ZTCs under study show much smaller average loading values, but nearly twice higher adsorption energies toward D4 and D5. This observation can be well understood since the small pores of ZTCs make them more challenging to adsorb the sterically bigger cyclic structures in large quantities, but offer more CH- π interactions between the cyclic methylsiloxanes and the delocalized π carbon framework of ZTC, leading to the enhanced adsorption energies. Thus, more attention will be paid to the loading capacity when evaluating ZTCs as sorbents for cyclic siloxanes. In other words, the best sorbent toward a cyclic contaminant is of the largest loading

S. Lin et al. / Green Energy & Environment xxx (xxxx) xxx

Table 2 Average loadings (L; per 10 nm³) and average adsorption energies (E; kcal mol⁻¹) of ZTCs with top 30% loading and adsorption performance toward both D4 and D5

	FAU1		FAU3		EMT	
	L per 10 nm ³	E kcal mol ⁻¹	L per 10 nm ³	E kcal mol ⁻¹	L per 10 nm ³	E kcal mol ⁻¹
D4	6.54	35.57	7.24	35.52	6.72	34.21
D5	4.88	38.66	4.99	37.42	5.29	39.01

values among those with top category adsorption energies (top 30% in this work; Tables S12 and S13).

FAU2 is the best sorbent for D4, which has the second-highest adsorption loading of 9.87 per 10 nm³ and fifth-highest adsorption energy of 38.15 kcal mol⁻¹, followed by FAU3 (7.24 per 10 nm³ loading, and 35.52 kcal mol⁻¹ adsorption energy), which has essentially similar structure but different pore sizes. For D5, the best ZTC is H8326849 structure with a fourth-highest loading of 6.20 per 10 nm³ and adsorption energy of 37.98 kcal mol⁻¹, followed by H8326896 with a slightly less adsorption loading and energy (5.83 per 10 nm³ and 37.74 kcal mol⁻¹, respectively).

3.2. Screening multi-functional ZTCs for linear/cyclic methylsiloxanes and derivatives

Notably, the top-performing ZTCs toward different contaminants are not the same due to the differences in the size, shape, and composition of the problematic compounds (PCs). If the diameters of pores or channels are much larger than the size of a PC, the adsorption energy will be much smaller; if the diameters of pores or channels are too small, the adsorption loading will be very low. Containing holes and channels with different sizes, it is very likely that some ZTCs can be effective sorbents for more than one methylsiloxane and derivative.

To screen multi-functional ZTCs, first, we set the strict criteria - top 30% in both adsorption energy and adsorption loading. Encouragingly, three out 68 ZTCs under investigation, namely FAU1, FAU3, and EMT (Table 2), meet our requirements for both cyclic methylsiloxanes (D4 and D5), and their loading and adsorption capabilities are rather satisfactory (loading > 4.9 per 10 nm³; adsorption energy > 34.2 kcal mol⁻¹). However, none of these ZTC structures can satisfy the above strict criteria as sorbents for all

the four linear contaminants. Therefore, no ZTC structures were in the top 30% for all the contaminants under examination, which demonstrates that ZTCs have more adsorption selectivity toward linear contaminants than cyclic contaminants.

Then, we lowered our screening criteria and identified the ZTCs with top 50% loading and adsorption capabilities toward each contaminant. Following these criteria, 10 out of 68 ZTCs are promising multi-functional sorbents for linear contaminants, and 18 ZTCs meet our standards as sorbents for the targeted cyclic siloxanes. Encouragingly, four top ZTCs, namely ISV, FAU1, FAU3, and H8326836 (Table 3), are of the top 50% performance for both linear and cyclic contaminants. Among these four top ZTCs, ISV has the highest average adsorption energy values toward all the six contaminants; FAU1 also has an outstanding performance as indicated by the largest loading capacities for all the contaminants; FAU3 possesses the top 30% loading and adsorption energy values towards D4 and D5, and is in the top 25% for DMSD; The ZTC H8326836 is in the top 30% for the loading towards methylsiloxanes and derivatives. Therefore, ISV, FAU1, FAU3, and H8326836 are multi-functional sorbents toward all the six contaminants and possess their own specific adsorption capability for different methylsiloxanes and derivatives. Note that several ZTCs have already been synthesized [41,42], we strongly believe that these four multi-functional adsorbents can be realized in the very near future, and have a good promise to be directly used as sorbents, without any functionalization or assembly with other adsorbents.

Compared with most adsorbents with relatively low affinities, ISV clearly distinguishes itself as an exceptional sorbent toward methylsiloxanes and derivatives. For linear contaminants, the predicted adsorption capacities of ISVtowards TMS (358 mg g⁻¹) and DMSD (407 mg g⁻¹) are about one to two orders of magnitude higher than our experimentally measured

Table 3 Average loadings (L; per 10 nm³) and average adsorption energies (E; kcal mol⁻¹) of the top four multi-functional ZTCs toward each contaminant at the pressure of 101.13 KPa.

	ISV		FAU1		FAU3		H8326836	
	L per 10 nm ³	E kcal mol ⁻¹	L per 10 nm ³	E kcal mol ⁻¹	L per 10 nm ³	E kcal mol ⁻¹	L per 10 nm ³	E kcal mol ⁻¹
DMSO ₂	33.07	18.69	34.03	17.52	36.74	17.47	33.70	17.76
TMS	24.14	18.28	25.39	17.81	24.87	16.47	24.14	16.75
DMSD	26.90	17.21	29.31	16.81	32.25	17.64	28.40	17.24
MMST	33.62	18.83	34.49	17.77	36.99	17.70	33.82	18.02
D4	4.87	34.64	6.54	35.57	7.24	35.52	5.83	33.77
D5	1.80	41.89	4.89	38.66	4.99	37.42	3.07	34.50

Please cite this article as: S. Lin et al., Zeolite-templated carbons as effective sorbents to remove methylsiloxanes and derivatives: A computational screening, Green Energy & Environment, https://doi.org/10.1016/j.gee.2020.07.007

DMSO₂

DMSD

25000

15000 20000

Pressure (kPa)

S. Lin et al. / Green Energy & Environment xxx (xxxx) xxx

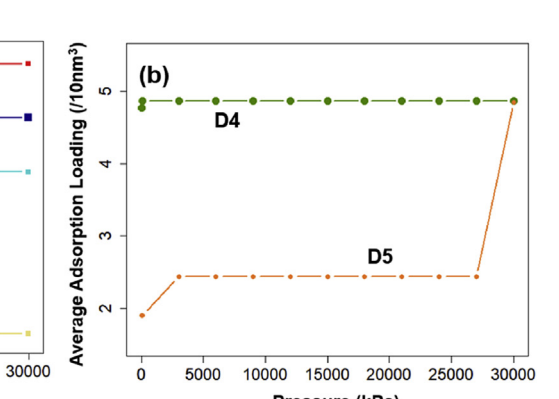


Fig. 2. Adsorption isotherm of (a) linear methylsiloxanes (DMSO₂, TMS, DMSD, and MMST), and (b) cyclic methylsiloxanes (D4 and D5) in ZTC ISV.

loadings (35 and 2 mg g⁻¹, respectively) of the activated carbon (Darco KB-G) (for details, see Fig. S2 in the Supporting Information). When the cyclic contaminants D4 and D5 are concerned, the predicted adsorption capacity toward D4 (237 mg g⁻¹) is twice as that of activated carbon in N₂ gas matrix (90 mg g⁻¹), and its loading toward D5 (110 mg g⁻¹) is close to experimentally measured loading of activated carbons (169 mg g⁻¹) [56]. Though the experimental conditions are more complicated, and the computational simulations are idealized, the above comparison between the predicted and measured loadings towards different contaminants does give us some evidence for the good promise of these sorbent materials.

5000

10000

Average Adsorption Loading (/10nm³)

28 30

26

(a)

To further explore the adsorption performance of ISV, we calculated its adsorption isotherms for the six contaminants. Fig. 2 presents the average loading of the contaminants in the ZTCs at different pressures. The adsorption isotherms of TMS, DMSO₂, and D4 remain the specific values within the pressure

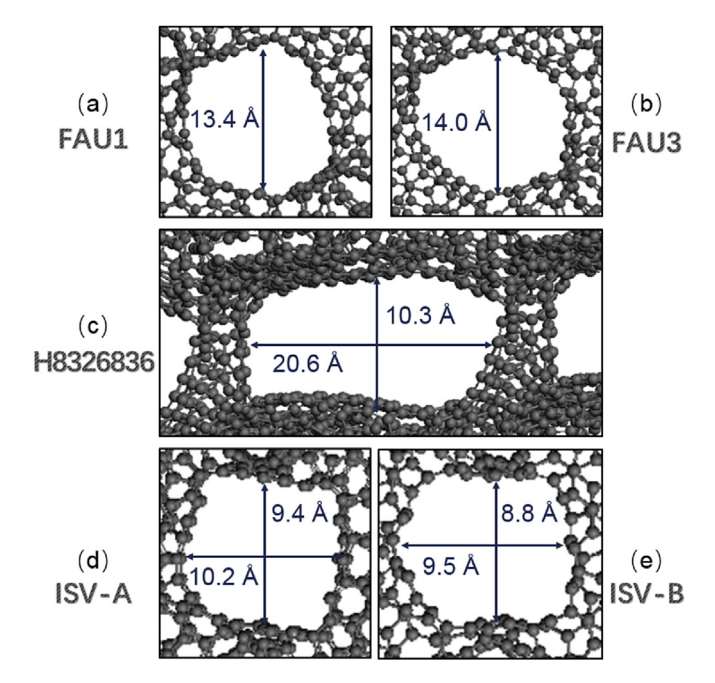


Fig. 3. Pore openings of the top four ZTCs: (a) FAU1, (b) FAU3, (c) H8326836, (d) ISV-opening A, and (e) ISV-opening B.

range of 3 MPa-30 MPa, and the average loading values are only slightly less at pressure lower than 3 MPa. For MMST and DMSD, as the pressure increases from 10 kpa to 3 MPa, the adsorbed contaminant increases from 33 to 34 per 10 nm³ and from 25 to 29 per 10 nm³, respectively, and the average loading keeps roughly the same value with increasing the pressure up to 12 MPa. When the pressure increases from 12 MPa to 18 MPa, the amount of contaminant adsorbed on MMST and DMSD increases from 34 to 36 per 10 nm³ and 29 to 32 per 10 nm³, respectively, and further pressure increase up to 30 MPa does not increase the average adsorption loading. The adsorption isotherm of D5 has a plateau of 2.4 per 10 nm³ between 3 MPa and 27 MPa, and it increases again at 30 MPa to 4.6 per 10 nm³, which is possible to be steady at a higher pressure. The adsorption isotherms provide the change of adsorption capabilities of ISV along with the transformation of the pressures. Note that ISV performs well at standard atmospheric pressure (101.33 kPa) with 33.07, 24.14, 26.90, 33.62, 4.87, and 1.80 per 10 nm³ adsorption loading for six methylsiloxanes and derivatives, and further increasing the pressures does not significantly improve the adsorption ability, especially in the typical operation pressure range.

3.3. The adsorption mechanism of ISV toward methylsiloxanes and derivatives

Our above studies revealed that ISV is the best-performing multi-functional sorbent toward all the six contaminants. What is the underlying adsorption mechanism? Note that the guidelines learned from such mechanisms can greatly facilitate our process to rationally design high-performance sorbents [37], and can also be integrated into the machine learning techniques to screen out promising sorbents with high efficiency [34].

To analyze the effect of pore geometries of ZTCs on the adsorption performance toward methylsiloxanes, we first examined the sizes of the six contaminants. For linear contaminants, the largest molecular length for DMSO $_2$ is ca. 4.50 Å, and the corresponding values for other linear contaminants, namely TMS, DMSD, and MMST, are about 4.92, 4.92, and 4.74 Å, respectively. As the cyclic methylsiloxanes are concerned, D4 and D5 have heights close to the diameter

of linear counterparts (4.06 and 4.91 Å, respectively), but their lengths (ca. 7.07 and 9.14 Å, respectively) are much larger. Generally, all the 68 ZTCs under investigation have sufficiently large pore sizes to adsorb both linear and cyclic methylsiloxanes and derivatives.

We then carefully studied the dominant pore properties of the four best-performing multi-functional ZTCs, namely ISV, FAU1, FAU3, and H8326836 (Fig. 3), since the relative size/ topology of the ZTC pores and the contaminant molecules determines the steric hindrance.

The pores of FAU1 and FAU3 are both spherical, and their diameters (ca. 13.4 and 14.0 Å, respectively) make them well host cyclic methylsiloxanes. Note that due to the relatively smaller pore size, FAU1 adsorbs the contaminants slightly stronger when compared with FAU3. The structure of ZTC H8326836 (Fig. 3) resembles layers of carbon structures connected by carbon tubes. In the flat layers, there are circular openings into the pores, and the connection of the layers by the tubes forms larger rectangular openings (ca. $20.6 \, \text{Å} \times 10.3 \, \text{Å}$), which are close to the circular openings and

play more important roles for adsorbing contaminants. The rather large pore sizes make FAU1, FAU3, and H8326836 well accept cyclic methylsiloxanes, while the corner of pores and the channels in their frameworks are beneficial to the adsorption of smaller linear methylsiloxanes and derivatives.

In comparison, ISV has various kinds of pore openings as well as numerous channels with different sizes in all the x, y and z directions, which help enhance adsorptions toward different methylsiloxanes and derivatives. Most of the pores in ISV are in square shapes, and their sizes are in a rather large range of 8.8-10.66 Å. Two types of dominant pores have dimensions of about 9.4×10.2 Å (pore A,Fig. 3d) and 8.8×9.5 Å (pore B, Fig. 3e), which are ideal for adsorbing cyclic containments. In short, it is the combination of different pores and channels that reduces the steric hindrance and enhances the adsorption toward methylsiloxanes and derivatives with different sizes, resulting in the best multi-functional ZTC for removing all the six containments.

Furthermore, we investigated the most favorable adsorption sites of the six contaminants inside ISV, the best-performing

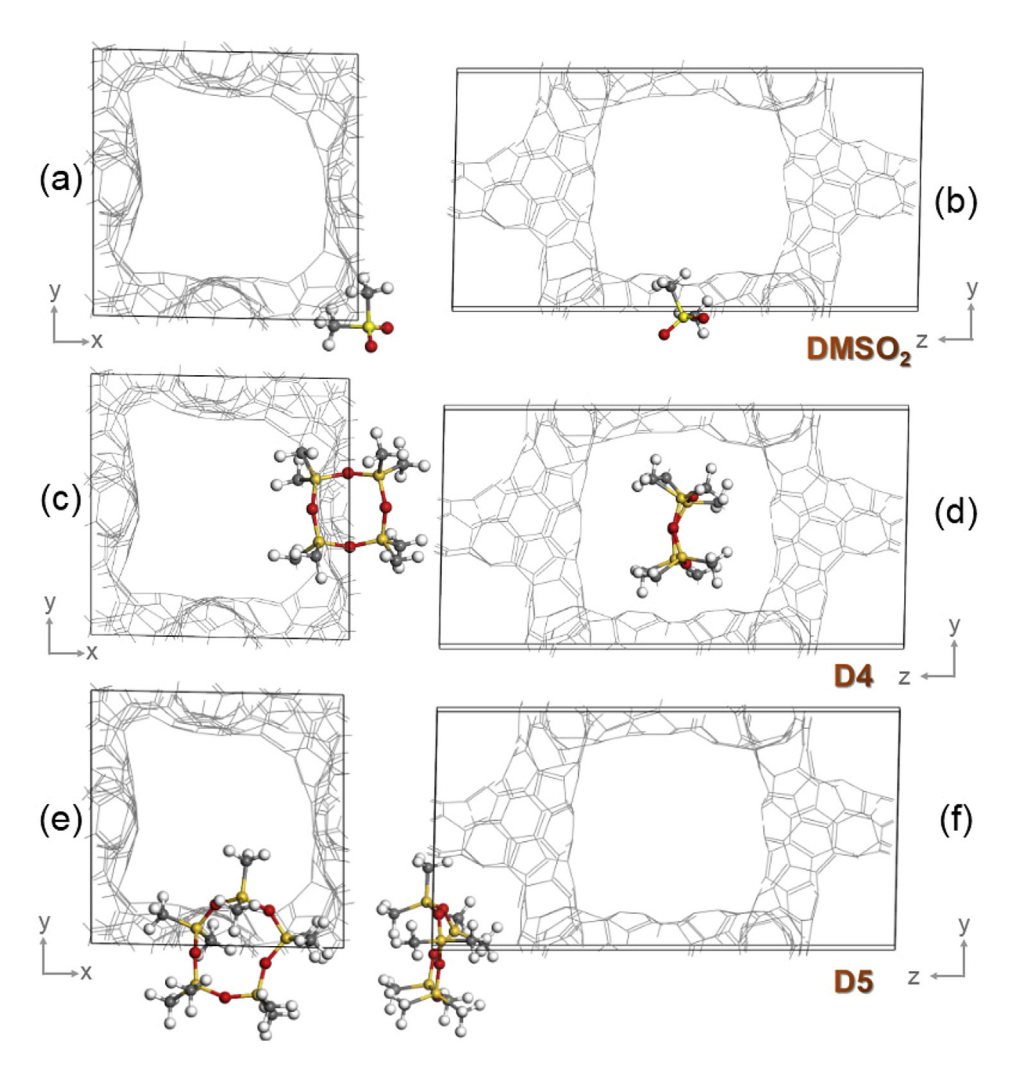


Fig. 4. Most favorable adsorption geometries of DMSO₂, D4, and D5 with ISV in the xy plane (a, c and e) and the yz plane (b, d, and f). The structures of ISV are presented in gray lines, and the structures of DMSO₂, D4 and D5 are presented as the ball-stick model. The yellow, red, khaki, and white balls stand for silicon, oxygen, sulfur, and hydrogen atoms, respectively.

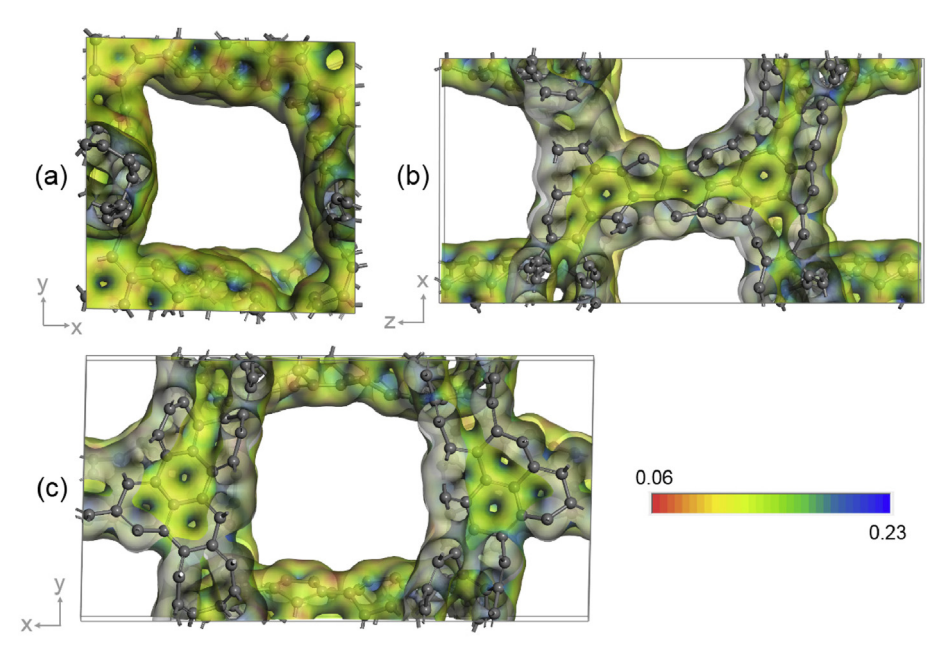


Fig. 5. Surface electrostatic potentials of ZTC-ISV in (a) the xy plane, (b) the xz plane, and (c) the yz plane. Gray balls stand for carbon atoms.

ZTC serving as a good representative of ZTCs. For this purpose, we performed GCMC simulations with fix-loading (one contaminant per supercell). Note that each contaminant has its own preferred adsorption position (Fig. 4). DMSO₂ prefers adsorption in the lower right corner in the *xy* plane of ISV (Fig. 4a), which is also the down middle site in the *yz* plane. Similarly, the other three linear methylsiloxanes and derivatives also tend to be adsorbed at the corners of small pores in the *xy*/*yz* plane. In comparison, cyclic methylsiloxanes, D4

and D5, occupy different positions due to their larger molecular volumes: D4 suits with the right side in the xy plane (Fig. 4c), which is the big hole in the center of yz plane (Fig. 4d), while D5 sits in the downside in the xy plane (Fig. 4e) and the hole in the corner in the yz plane (Fig. 4f).

The electrostatic interaction and charge transfer also play critical roles for the adsorption capacity of adsorbents toward containments. Thus, we performed DFT computations based on the ISV structure containing one contaminant per supercell.

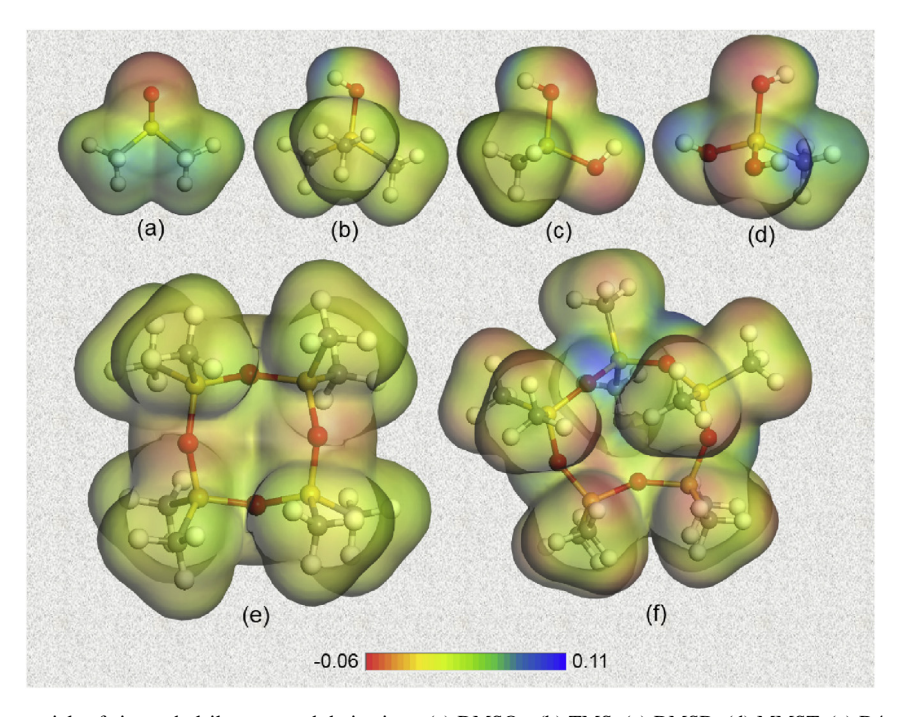


Fig. 6. Surface electrostatic potentials of six methylsiloxanes and derivatives: (a) DMSO₂, (b) TMS, (c) DMSD, (d) MMST, (e) D4, and (f) D5. The yellow, light yellow, gray and white balls represent silicon, sulfur, carbon and hydrogen atoms, respectively.

The ISV generally shows slightly positive electrostatic potential, with the electrostatic values ranging from 0.06 to 0.23 (Fig. 5). Note that on the surfaces of the six methylsiloxanes and derivatives, the O atoms show negative electrostatic potentials, while the H atoms bonding to O atoms present more positive electrostatic potentials than other atoms (Fig. 6). Therefore, the O atoms tend to bind with ISV due to electrostatic interactions.

We examined the charge transfer between ISV and the contaminants by comparing the Hirschfeld charges before and after adsorption. In general, all the adsorbed contaminants behave as electron acceptors, i.e., the adsorbed methylsiloxanes and derivatives attain the electrons from ZTCs. The most significant charge transfer occurs on D4 and D5, 0.33 and 0.37 e, respectively, which echo the strong interactions between cyclic methylsiloxanes and ZTCs. Among linear contaminants, TMS and DMSD have more significant charge transfers, both obtain 0.14 e from ISV, while DMSO₂ and MMST gain some fewer electrons (0.07 and 0.09 e) from the sorbent. The electron acceptor characteristic of the contaminants originates from the strong electronegativity of oxygen atoms in methylsiloxanes. Thus, oxygen atoms on the methylsiloxanes play dominant roles for the absorption in ZTCs. Note that the charge transfer can further enhance the electrostatic interactions between ZTCs and the contaminants under this

Another factor that enhances the adsorption performance of ISV toward methylsiloxanes and derivatives is the abundance of CH- π bonds between them. All six containments have a high density of -CH₃ groups. Meanwhile, ISV consists of graphene nanochannels, on which π electrons are well delocalized. Therefore, the C-H bonds in the -CH₃ groups can interact with the free π electron cloud on the surface of ISV, and the resulting CH- π interactions help improve the adsorption of methylsiloxanes and derivatives.

In summary, steric hindrance, electrostatic interactions (further enhanced by charge transfer), and $CH-\pi$ interactions are essential factors for increase the adsorption capabilities of ZTCs toward methylsiloxanes and derivatives, which are in line with our previous finding based on zeolite sorbents [37].

4. Conclusion

In this work, by means of GCMC simulations and DFT computations, we explored the potentials of 68 stable ZTCs to remove cyclic and linear siloxanes. Our GCMC simulations identified several ZTCs as promising sorbents for removing cyclic siloxanes, D4 and D5, and four linear methylsiloxanes and derivative, namely DMSO₂, TMS, DMSD, and MMST. Specifically, we screened out four multi-functional ZTCs with the exceptional overall performances, namely ISV, FAU1, FAU3, and H8326836, which can firmly adsorb all the six methylsiloxanes with rather high loading values, especially for D4: its adsorption capacity toward D4 (237 mg g⁻¹) is twice as that of activated carbon in N₂ gas matrix (90 mg g⁻¹) [56]. Notably, ISV is expected to perform best: it has the highest average adsorption energies toward all the six contaminants,

and its excellent performance well remains at even very high pressure. Our careful analyses revealed that pore sizes and distributions, electrostatic interactions, and CH- π interactions are dominant factors for the enhanced interactions between containments and adsorbents.

This study not only identified most promising ZTCs as adsorbents toward the removal of methylsiloxanes and derivatives for future experimental explorations but also demonstrated the efficiency of the computational screening procedure, which paves the way to screen more ZTCs and related materials as sorbents to remove problematic compounds.

Declaration of competing interest

The authors declare no conflict of interest.

Acknowledgment

work was financially supported by NASA (Grant80NSSC17M0047) and NSF (REU 1757365). This research used resources of the High Performance of Computational facility (HPCf), University of Puerto Rico, which is partially supported by an Institutional Development Award (IDeA) INBRE Grant Number P20GM103475 from the National Institute of General Medical Sciences (NIGMS), a component of the National Institute of Health (NIH), and the Bioinformatics Research Core of the INBRE. Its contents are solely the responsibility of the authors and do not necessarily represent the official view of NIH. A portion of the calculations used the resources of the Compute and Data Environment for Science (CADES) at ORNL and of the National Energy Research Scientific Computing Center, which are supported by the office of science of the U.S. DOE under Contract No. DE-AC05-00OR22750 and DE-AC02-05CH11231, respectively.

Appendix A. Supplementary data

Supplementary data to this article can be found online at https://doi.org/10.1016/j.gee.2020.07.007.

References

- [1] A. Divsalar, H. Divsalar, M.N. Dods, R.W. Prosser, T.T. Tsotsis, Ind. Eng. Chem. Res. 58 (2019) 16502.
- [2] B. Tansel, S.C. Surita, Waste Manag. 96 (2019) 121-127.
- [3] C.-U. Bak, C.-J. Lim, J.-G. Lee, Y.-D. Kim, W.-S. Kim, Separ. Purif. Technol. 209 (2019) 542–549.
- [4] C. Rauert, T. Harner, J.K. Schuster, A. Eng, G. Fillmann, L.E. Castillo, O. Fentanes, M.N. Villa Ibarra, K.S. Miglioranza, I. Moreno Rivadeneira, Environ. Sci. Technol. 52 (2018) 7240–7249.
- [5] E. Santos-Clotas, A. Cabrera-Codony, B. Ruiz, E. Fuente, M.J. Martín, Bioresour. Technol. 275 (2019) 207–215.
- [6] A.S. Calbry-Muzyka, A. Gantenbein, J. Schneebeli, A. Frei, A.J. Knorpp, T.J. Schildhauer, S.M. Biollaz, Chem. Eng. J. 360 (2019) 577–590.
- [7] Y. Lu, T. Yuan, W. Wang, K. Kannan, Environ. Pollut. 159 (2011) 3522– 3528

- [8] L. Zhi, L. Xu, X. He, C. Zhang, Y. Cai, Sci. Total Environ. 631 (2018) 879-886
- [9] J. Velicogna, E. Ritchie, J. Princz, M.-E. Lessard, R. Scroggins, Chemosphere 87 (2012) 77-83.
- [10] V.T.L. Tran, P. Gélin, C. Ferronato, P. Mascunan, V. Rac, J.-M. Chovelon, G. Postole, Chem. Eng. J. 371 (2019) 821-832.
- [11] A.A. Bletsou, A.G. Asimakopoulos, A.S. Stasinakis, N.S. Thomaidis, K. Kannan, Environ. Sci. Technol. 47 (2013) 1824-1832.
- [12] C. Sparham, R. Van Egmond, S. O'connor, C. Hastie, M. Whelan, R. Kanda, O. Franklin, J. Chromatogr, A 1212 (2008) 124-129.
- [13] W.J. Hong, H. Jia, C. Liu, Z. Zhang, Y. Sun, Y.F. Li, Environ. Pollut. 191 (2014) 175-181.
- [14] S. Genualdi, T. Harner, Y. Cheng, M. Macleod, K.M. Hansen, R. Van Egmond, M. Shoeib, S.C. Lee, Environ. Sci. Technol. 45 (2011) 3349-3354
- [15] C. Sánchez-Brunete, E. Miguel, B. Albero, J.L. Tadeo, J. Chromatogr, A 1217 (2010) 7024-7030.
- [16] E.C. Tuazon, S.M. Aschmann, R. Atkinson, Environ. Sci. Technol. 34 (2000) 1970-1976.
- [17] J.A. Rutz, J.R. Schultz, C.M. Kuo, H.E. Cole, S. Manuel, M. Curtis, P.R. Jones, O.D. Sparkman, J.T. Mccoy, in: 41st International Conference on Environmental Systems, vol. 17, AIAA, Portland, Oregon, 2011, p. 5154.
- [18] T. Rector, C. Metselaar, B. Peyton, J. Steele, W. Michalek, E. Bowman, M. Wilson, D. Gazda, L. Carter, in: 44th International Conference on Environmental Systems, AIAA, Tucson Arizona, 2014.
- [19] L. Carter, J. Perry, M.J. Kayatin, M. Wilson, G.J. Gentry, E. Bowman, O. Monje, T. Rector, J. Steele, in: 45th International Conference on Environmental Systems, AIAA, Bellevue, Washington, 2015.
- [20] J.A. Rutz, J.R. Schultz, C.M. Kuo, M. Curtis, P.R. Jones, O.D. Sparkman, J.T. Mccoy, AIAA Technical Paper. (2011) 1021758.
- [21] D.L. Carter, E.M. Bowman, M.E. Wilson, T.J. Rector, 43rd International Conference on Environmental Systems. (2013) 3510.
- [22] D.L. Carter, B. Tobias, N.Y. Orozco, 43rd International Conference on Environmental Systems. (2013) 3509.
- [23] T. Rector, C. Metselaar, B. Peyton, J. Steele, W. Michalek, E. Bowman, M. Wilson, D. Gazda, L. Carter, An Evaluation of Technology to Remove Problematic Organic Compounds from the International Space Station Potable Water (2014).
- [24] D.-G. Wang, M. Aggarwal, T. Tait, S. Brimble, G. Pacepavicius, L. Kinsman, M. Theocharides, S.A. Smyth, M. Alaee, Water Res. 72 (2015) 209-217.
- [25] J. Sanchís, E. Martínez, A. Ginebreda, M. Farré, D. Barceló, Sci. Total Environ. 443 (2013) 530-538.
- [26] M.M. Coggon, B.C. Mcdonald, A. Vlasenko, P.R. Veres, F.O. Bernard, A.R. Koss, B. Yuan, J.B. Gilman, J. Peischl, K.C. Aikin, Environ. Sci. Technol. 52 (2018) 5610-5618.
- [27] L. Xu, S. Xu, L. Zhi, X. He, C. Zhang, Y. Cai, Environ. Sci. Technol. 51 (2017) 12337-12346.
- [28] L. Zhi, L. Xu, Y. Qu, C. Zhang, D. Cao, Y. Cai, Environ. Sci. Technol. 52 (2018) 12235-12243.

- [29] X. Wang, J. Schuster, K.C. Jones, P. Gong, Atmos. Chem. Phys. 18 (2018) 8745-8755.
- [30] I.S. Krogseth, X. Zhang, Y.D. Lei, F. Wania, K. Breivik, Environ. Sci. Technol. 47 (2013) 4463-4470.
- [31] J. Sanchís, A. Cabrerizo, C. Galbán-Malagón, D. Barceló, M. Farré, J. Dachs, Environ. Sci. Technol. 49 (2015) 4415-4424.
- [32] J.V. Sousa, P.C. Mcnamara, A.E. Putt, M.W. Machado, D.C. Surprenant, J.L. Hamelink, D.J. Kent, E.M. Silberhorn, J.F. Hobson, Environ. Toxicol. Chem Int. J. 14 (1995) 1639-1647.
- [33] M. Tong, Y. Lan, Q. Yang, C. Zhong, Green Energy Environ 3 (2018) 107-119
- [34] B. Wang, L.H. Xie, X. Wang, X.M. Liu, J. Li, J.R. Li, Green Energy Environ 3 (2018) 191-228.
- [35] S. Xu, B. Kropscott, Anal. Chem. 84 (2012) 1948–1955.
- [36] S. Lin, Y. Wang, Y. Zhao, L. Pericchi, A.J. Hernandez-Maldonado, Z. Chen, J. Mater, Chem, A 8 (2020) 3228-3237.
- [37] X. Wei, Y. Wang, A.J. Hernández-Maldonado, Z. Chen, Green Energy Environ. 2 (2017) 363-369.
- [38] H. Nishihara, T. Kyotani, Adv. Mater. 24 (2012) 4473-4498.
- [39] W. Gu. G. Yushin, Wires, Energy Environ, 3 (2014) 424-473.
- [40] T. Roussel, A. Didion, R.J.-M. Pelleng, R. Gadiou, C. Bichara, C. Vix-Guterl, J. Phys, Chem. C 111 (2007) 15863-15876.
- [41] H. Lee, K. Kim, S.H. Kang, Y. Kwon, J.H. Kim, Y.K. Kwon, R. Ryoo, J.Y. Park, Sci. Rep. 7 (2017) 1-9.
- [42] E. Braun, Y. Lee, S.M. Moosavi, S. Barthel, R. Mercado, I.A. Baburin, D.M. Proserpio, B. Smit, Proc. Natl. Acad. Sci. 115 (2018) E8116-
- [43] H. Nishihara, H. Fujimoto, H. Itoi, K. Nomura, H. Tanaka, M.T. Miyahara, P.A. Bonnaud, R. Miura, A. Suzuki, N. Miyamoto, Carbon. 129 (2018) 854-862.
- [44] K. Nueangnoraj, H. Nishihara, K. Imai, H. Itoi, T. Ishii, M. Kiguchi, Y. Sato, M. Terauchi, T. Kyotani, Carbon. 62 (2013) 455-464.
- [45] H. Nishihara, Q.-H. Yang, P.-X. Hou, M. Unno, S. Yamauchi, R. Saito, J.I. Paredes, A. Martínez-Alonso, J.M. Tascón, Y. Sato, Carbon. 47 (2009) 1220-1230.
- [46] K. Kim, T. Lee, Y. Kwon, Y. Seo, J. Song, J.K. Park, H. Lee, J.Y. Park, H. Ihee, S.J. Cho, Nature. 535 (2016) 131.
- [47] J. Parmentier, F.O. Gaslain, O. Ersen, T.A. Centeno, L.A. Solovyov, Langmuir. 30 (2014) 297-307.
- [48] I. Accelrys, Accelrys Software Inc. (2010).
- [49] W.K. Hastings, Biometrika 57 (1970) 97-109.
- [50] H. Sun, J. Phys, Chem. B 102 (1998) 7338-7364.
- [51] H. Sun, P. Ren, J. Fried, Comput. Theor. Polym. Sci. 8 (1998) 229-246.
- [52] B. Delley, J. Chem, Phys. 92 (1990) 508-517.
- [53] B. Delley, J. Chem, Phys. 113 (2000) 7756-7764.
- [54] J.P. Perdew, K. Burke, M. Ernzerhof, Phys. Rev. Lett. 77 (1996) 3865.
- [55] S. Grimme, J. Comput, Chem. 27 (2006) 1787-1799.
- [56] S. Nam, W. Namkoong, J.-H. Kang, J.-K. Park, N. Lee, Waste Manag. 33 (2013) 2091-2098.